Understanding the Antitumor Activity of Novel Hydroxysemicarbazide Derivatives as Ribonucleotide Reductase Inhibitors Using CoMFA and CoMSIA

Anand V. Raichurkar and Vithal M. Kulkarni*,†

Pharmaceutical Division, Institute of Chemical Technology, University of Mumbai, Matunga, Mumbai-400019, India

Received January 8, 2003

Three-dimensional quantitative structure−activity relationship (3D-QSAR) studies were performed on a series of Schiff bases of hydroxysemicarbazide analogues using comparative molecular field analysis (CoMFA) and comparative molecular similarity indices analysis (CoMSIA) methods with their antitumor activities against L1210 cells. The models were generated using 24 molecules, out of which one molecule was a commercially available ribonucleotide reductase (RR) inhibitor, hydroxyurea (HU), and the predictive ability of the resulting each model was evaluated against a test set of four molecules. Maximum common substructure (MCS)-based method was used for alignment and compared with the known alignment methods. The QSAR models from both methods exhibited considerable correlative and predictive properties. Inclusion of additional descriptor ClogP improved the statistics of CoMFA model significantly. Both methods strongly suggest the necessity of lipophilicity for antitumor activity. CoMFA and CoMSIA methods predicted HU optimally, indicating a similar mechanism of action for the molecules considered for generating the models and HU to inhibit the tumor cells. The analysis of CoMFA contour maps provided insight into the possible modification of the molecules for better activity.

Introduction

Among the devastating and pandemic diseases, cancer is a major disease and according to WHO, it is considered as the fourth largest killer disease. Treatment of cancer has been one of the primary goals of medicine for the last two decades. Though several therapies namely surgery, photodynamic therapy, radiation therapy, chemoimmunotherapy, gene therapy, and chemotherapy are available, chemotherapy is considered as an effective approach for combating cancer. However, in view of the lack of selectivity, increasing incidence of resistance to current drug regimens, and the frequency of adverse events, the development of novel, selective, potent, and safe antitumor agents that are also active against mutant cells has remained a high priority.

Ribonucleotide reductase (RR) is a key enzyme, which plays a major role in the DNA synthesis and repair in all dividing cells.[1] It catalyzes the reduction of ribonucleotides and provides the building blocks for the de novo DNA synthesis. Various biological and experimental studies have indicated the critical role of RR in neoplastic expression and tumor promotion. Therefore, RR is considered as a relevant molecular target for the design and development of antitumor agents.[2]

Several compounds with hydroxyguanidine, thiosemicarbazide, and substituted benzohydroxamic acid functional groups have shown promising RR inhibitory property with antitumor activity.[3−5] On the basis of previous reports, it is believed that (−C(=X)NHOH; X = O, NH) is an essential pharmacophore for antitumor/antiviral activities.[6] Hydroxyurea (HU) and triapine, which inhibit RR, have emerged commercially as antitumor agents, and recently RR inhibitors have additionally shown antiviral activities and hence are used in the treatment of AIDS as an adjuvant therapy.[7−10] The dual therapeutic activities, antitumor and antiviral, of RR inhibitors have made RR as one of the promising targets for the design and development of novel drugs.

In the search of more potent and selective antitumor agents, Ren et al. synthesized a series of Schiff bases of hydroxysemicarbazide (SB−HSC) with the essential pharmacophore (NHCONHOH) and tested them for antitumor activity against L1210 cancer cells.[11] The compounds were synthesized with a view to understand the role of aryl group and substitution pattern that affect antitumor activity. This resulted in a data set of compounds with a wide spectrum of activities. Though the compounds were tested against L1210 cancer cells, Ren et al. hypothesized that the presence of the pharmacophore, which is also present in HU, may induce the observed activity by inhibiting the RR enzyme. However, there was no experimental evidence for this hypothesis. Therefore, to rationalize the observed variance in the biological activity, to propose a possible mechanism of antitumor activity as a further support to the hypothesis of Ren et al., and to guide the synthesis of additional compounds, we have derived three-dimensional quantitative structure−activity relationship (3D-QSAR) models for SB−HSC derivatives using comparative molecular field analysis (CoMFA) and comparative molecular similarity indices analysis (CoMSIA) methods. These methods were applied in the past to various therapeutic areas in our laboratory.[12−14]

The 3D-QSAR, CoMFA method was proposed by Cramer et al. in 1988, which is extensively used in the present practice of drug discovery.[15] One of the advan-

* To whom correspondence should be addressed. Tel: +91−22−24186718. Fax: +91−22−24145614. E-Mail: vithal@biogate.com.

† Present address: Bharati Vidyapeeth Deemed University, Poona College of Pharmacy, Pune-411008, India. E-mail: vmkulkarni60@yahoo.co.in.

10.1021/jm030016a CCC: $25.00
Published on Web 09/13/2003

tages of CoMFA is the ability to predict the biological activity of the molecules by deriving a relation between steric/electrostatic properties and biological activities in the form of contour maps. Several improvements have been made in alignment methodology: addition of macroscopic descriptor(s) in the study table and recently a reverse method of CoMFA, called AFMoC (adaptation of fields for molecular comparison) and topomer CoMFA have been introduced.[16−19]

The CoMSIA method of 3D-QSAR was introduced by Klebe in 1994 in which a common probe atom and similarity indices are calculated at regularly spaced grid points for the prealigned molecules.[20] The distance-dependence between the probe atom and the molecule atoms is determined by Guassian function through similarity indices calculated at all grid points. The CoMSIA considers five different property fields: steric, electrostatic, hydrophobic, hydrogen bond donor (H bond donor) and acceptor (H bond acceptor). The advantage of this method over CoMFA is that it provides additional fields, particularly hydrophobicity of compounds.

Herein, we report application of two 3D-QSAR methods, CoMFA and CoMSIA, aimed to understand the antitumor activity of SB−HSC derivatives and to compare both with respect to their predictive power. We have also analyzed the structural requirements of RR inhibitors as antitumor agents in terms of steric, electrostatic, lipophilic, and hydrogen bond donor and acceptor properties using these methods. Such information is essential to understand the SAR of SB−HSC derivatives and subsequently for the design of potent antitumor agents.

Methods

Data Set for Analysis. Twenty-eight molecules selected for the present study were taken from the published work by Ren et al.[11] The structures of the compounds and their biological data are given in Table 1. Out of these molecules, 27 were Schiff bases of hydroxysemicarbazide derivatives, and molecule **24** was a commercially available RR inhibitor, hydroxyurea (HU). Ren et al. reported 30 SB−HSC out of which three molecules were found to have a different rate-limiting step from other compounds as inhibitors of the tumor cells. Thus 27 molecules were included, and three were deleted from the studies with a view that molecules considered for any 3D-QSAR studies must share a similar kind of mechanism of action. The 3D-QSAR models were generated using a training set of 24 molecules (compounds **1**−**24**, Table 1). Predictive power of the resulting models was evaluated using a test set of four molecules (compounds **25**−**28**, Table 1). The biological activity used in the present study was expressed as

$$pIC_{50} = -\log IC_{50}$$

where IC_{50} is the concentration (μM) of the inhibitor producing 50% inhibition of L1210 cancer cell lines.

Molecular Modeling. All computational studies were performed using SYBYL 6.6 software running on Silicon Graphics Indy R5000 workstation.[21] The compounds were built from fragments in the SYBYL database. Each structure was fully geometry-optimized using the standard Tripos force field with a distance-dependent dielectric function and a 0.001 kcal/mol Å energy gradient convergence criterion. Partial atomic charges required for calculation of the electrostatic interactions were computed by a semiempirical molecular orbital method using the MOPAC 6.0 program.[22] The charges were computed using the AM1 Hamiltonian within MOPAC 6.0.[23] Using the systemic search protocol, the conformational search on each SB−HSC analogue was performed by rotating all the rotational bonds from 0 to 359° by 10° increments. Conformational energies were computed with an electrostatic term. The lowest energy conformer obtained using a systematic search was minimized and used for alignment. The most active analogue (compound **21**) was used as the template for aligning the other analogues.

Alignment Rules. Superimposition of the molecules was carried out by the following alignments:

(1) Atom-based alignment: In this, atoms C═NNC(═O)NO of the molecules were used for rms fitting onto the corresponding atoms of the template structure. The atoms used for the alignment are marked with asterisk (*) in Figure 1a.

(2) Field fit alignment: This was carried out by using the SYBYL QSAR rigid body field fit command within SYBYL. The most active molecule was used as the template structure. Field fit adjusts the geometries of the molecules such that their steric and electrostatic fields match the fields of the template molecule.

(3) Maximum common substructure (MCS)-based alignment: Charisma module in SYBYL 6.6 performs the rigid alignment of molecules using MCS. It attempts to align molecules to a template molecule on a common backbone or core.

For each molecule to be aligned, (a) the core of the molecule is identified, and (b) the core may be found more than once or there may be more than one mapping of the core atoms to the molecule atoms. In this core a single mapping is chosen as follows:

(i) First, the rms deviation for each mapping is examined. The mapping with the lowest rms deviation is chosen.

(ii) If there is more than one mapping with the same rms deviation (mappings are considered the same when the difference in rms ratio is within 0.005), the mapping that produces the lowest differential volume between the molecule and the template is chosen.

(c) The molecule is fitted to the template using the best mapping of the core to the molecule.

Using Charisma, by ignoring the bond types in the rings, an MCS was determined which was subsequently used for alignment. MCS used in the current study is shown in Figure 1b.

CoMFA and CoMSIA Analysis. For each of the alignments, CoMFA steric and electrostatic fields were separately calculated at each lattice intersection on a regularly spaced grid of 2.0 Å units in all *X*, *Y*, and *Z* directions. The van der Waals potential and columbic terms, which represent the steric and electrostatic terms, respectively, were calculated using the standard Tripos force field. A distance dependent dielectric constant of 1.00 was used. An sp^3 carbon atom with a van der Waals radius of 1.52 Å and +1.0 charge was selected as the probe to calculate the steric and electrostatic fields. Values of the steric and electrostatic energy were truncated at 30 kcal/mol. The electrostatic contributions were ignored at the lattice intersection with maximal steric interactions.

CoMSIA calculates similarity indices at the intersections of a surrounding lattice. The same grid constructed for the CoMFA field was used for the CoMSIA fields calculation. The five CoMSIA fields available within SYBYL (steric, electrostatic, hydrophobic, hydrogen bond donor and acceptor) were calculated at the grid lattice point using a probe atom of 1 Å radius as well as the charge, hydrophobic and hydrogen bond properties of H, and an attenuation factor of 0.3.

PLS Analysis. The partial least-squares (PLS) analysis algorithm was used in conjugation with the cross-validation (leave-one-out) option to obtain an optimum number of components which were used to generate the final CoMFA model without cross validation. The result from a cross validation analysis was expressed as r^2_{cv} which is defined as

$$r^2_{cv} = 1 - \mathrm{PRESS}/\sum (Y - Y_{mean})^2$$

where

$$\mathrm{PRESS} = \sum (Y - Y_{pred})^2$$

Table 1. Structures and Biological Activities of Molecules Used in the Present Study

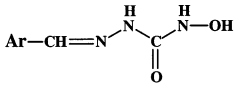

S. NO	Ar	pIC_{50}[a]	S. NO	Ar	pIC_{50}[a]
1	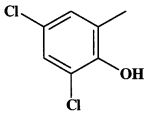	5.187	8	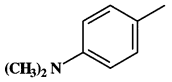	3.350
2	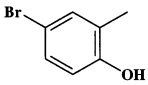	4.996	9	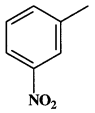	3.399
3	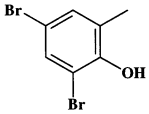	5.143	10	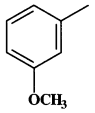	3.433
4	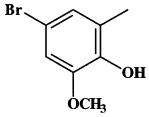	4.424	11	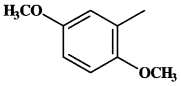	4.521
5	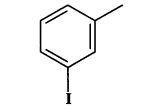	4.095	12	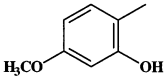	4.220
6	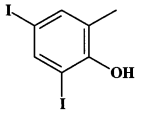	5.328	13	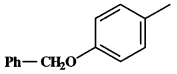	4.318
7	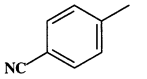	3.681	14	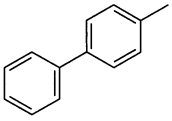	4.370
15	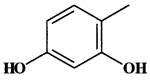	3.883	22	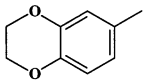	3.749
16		3.217	23	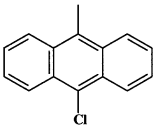	5.268
17	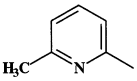	3.050	24	HNCONH-OH	4.086
18	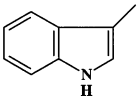	3.322	25*	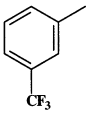	4.403
19	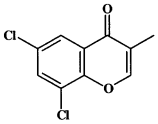	4.550	26*	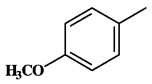	3.499
20	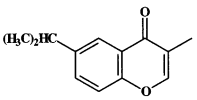	4.492	27*	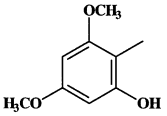	4.039
21	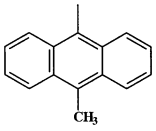	5.357	28*	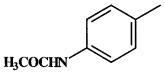	3.025

[a] Expressed as the logarithm of $1/IC_{50}$ (μM) value. *Test set molecules.

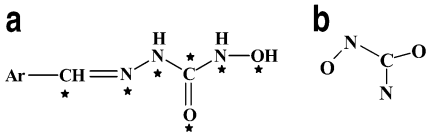

Figure 1. Atoms considered for aligning the molecules in different methods. (a) Atom-based fit. (b) Most common substructure (Charisma) fit.

Table 2. Summary of CoMFA Results with Different Alignment Methods

	analysis A		
	RMS	field fit	MCS
r^2_{cv}	0.583	0.073	0.359
SEP	0.533	0.935	0.660
components	5	10	5
r^2_{ncv}	0.949	0.998	0.945
SEE	0.187	0.013	0.194
r^2_{pred}	0.104	0.317	0.097

Predictive r^2 Values. To validate the derived models, biological activities of the test set molecules were predicted using models derived from training set. Predictive r^2 (r^2_{pred}) value was calculated using formula

$$r^2_{pred} = (SD - PRESS)/SD$$

where SD is the sum of squared deviations between the biological activity of the test set and the mean activity of training set molecules, and PRESS is the sum of squared deviations between the actual and the predicted activities of the test set molecules.

Results and Discussion

Two methods, CoMFA and CoMSIA, were used to derive 3D-QSAR models for SB−HSC derivatives as ribonucleotide reductase inhibitors with antitumor activity.[11] The in vitro data of antitumor activities determined against L1210 cancer cells were used as dependent variables in this study.

All the cross-validated results were analyzed by considering the fact that a value of r^2_{cv} above 0.3 indicates that the probability of chance correlation is less than 5%. Conformation of the molecules used in the study was searched using a systematic search method. Relative alignment of molecules was then carried out using three techniques, namely rms fit, SYBYL rigid body fit, and MCS fit methods.

The results obtained from the CoMFA studies are summarized in Tables 2 and 3. Analysis A (Table 2) shows results obtained from the three different alignments. The atom-based alignment exhibited a cross-validated r^2 (r^2_{cv}) of 0.583 with five components. A non-cross-validated r^2 (r^2_{ncv}) of 0.949 was observed with this model. However, the predictive ability of this model was poor (r^2_{pred} of 0.104). The field fit alignment showed even less r^2_{cv} of 0.073 with 10 components and has an r^2_{ncv} of 0.998. The predictive ability of this model was more than rms alignment but other statistics were insignificant. Realignment of the molecules by MCS method gave comparable PLS results as that of the rms alignment. The model was characterized by an r^2_{cv} of 0.359 at five components and an r^2_{ncv} of 0.945. However, this model also exhibited a poor r^2_{pred} of 0.097. On the basis of the predictive ability and other statistical parameters, out of the three CoMFA models (analysis A), the model generated using atom-based alignment was selected to improve the statistics of the present CoMFA model.

Table 3. Summary of Analysis of CoMFA Models Using Additional Descriptors[a]

	analysis B				
	ClogP	H	L	ClogP+H	ClogP+L
r^2_{cv}	0.708	0.520	0.514	0.680	0.692
SEP	0.473	0.588	0.592	0.680	0.519
components	7	6	6	7	9
r^2_{ncv}	0.993	0.969	0.968	0.991	0.996
SEE	0.072	0.149	0.151	0.082	0.057
F	336.64	88.81	86.36	258.16	421.28
r^2_{pred}	0.796	−0.194	−0.046	0.805	0.798
contribution					
steric	0.363	0.466	0.454	0.362	0.358
electrostatic	0.426	0.480	0.468	0.416	0.424
ClogP	0.211	- -	- -	0.216	0.211
HOMO	- -	0.054	- -	0.006	- -
LUMO	- -	- -	0.078	- -	0.007
r^2_{bs}	0.998	0.988	0.987	0.997	0.999
std dev	0.002	0.007	0.009	0.002	0.001

[a] H = HOMO, L = LUMO.

The activity data used in the present study was in vitro, and such a type of activity data could have contributions not only from steric and electrostatic fields but also from other physicochemical properties, particularly hydrophobicity of the molecules. These properties account for the transport phenomenon and for pharmacokinetic profile of the molecules. The authors in their original paper have performed classical-QSAR and found that the activity is influenced by lipophilicity of the molecules.[11] To account for the hydrophobic properties, which may influence this type of activity, ClogP was included in the analysis. As the rms method of alignment showed good statistical results, we decided to add an additional descriptor to this model. As assumed, inclusion of ClogP contributed significantly to the CoMFA model. Table 3 summarizes the results obtained from the CoMFA model after inclusion of the additional descriptors.

Analysis B (Table 3) shows that inclusion of ClogP improved the statistical significance of the model from r^2_{cv} 0.583 to 0.708, and r^2_{ncv} from 0.949 to 0.993. The standard error of estimate (SEE), a significant value of 0.072, is a measure of the target property still unexplainable by the resultant model. The higher F value (336.64) suggests that inclusion of ClogP is meaningful. This is supported by the fact that it is contributing up to 0.211 along with steric 0.363 and electrostatic 0.426 properties.

We have also calculated highest occupied molecular orbital (HOMO) and lowest occupied molecular orbital (LUMO) descriptors using MOPAC 6.0 program available in SYBYL, and these were added to the study table. The models were generated using HOMO, LUMO, or either of them in combination with ClogP in addition to CoMFA fields. The results are summarized in Table 3. Addition of HOMO or LUMO in combination with steric and electrostatic fields gave an r^2_{cv} of 0.52 and 0.514, respectively, at six components. The r^2_{ncv} of resultant models were more than 0.9 in each case, but the predictive ability of all models was very poor. We then added each descriptor individually along with CoMFA and ClogP descriptors. Here also inclusion of ClogP converted the poor statistical terms to significant ones, particularly the predictive ability of each model

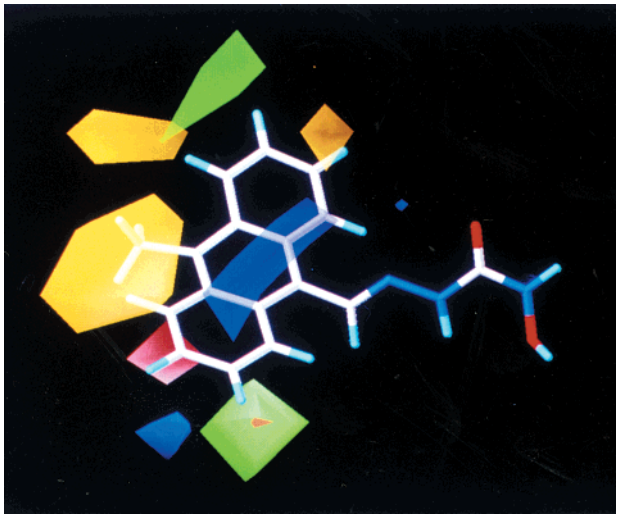

Figure 2. CoMFA steric and electrostatic STDEV*COEFF contour plots from atom- based alignment with ClogP as additional descriptor (Analysis B). Sterically favored areas (contribution level 80%) are represented by green polyhedra. Sterically disfavored areas (contribution level 20%) are represented by yellow polyhedra. Positive charge favored areas (contribution level 80%) are represented by blue polyhedra. Negative charge favored areas (contribution level 20%) are represented by red polyhedra. The most active compound **21** shown in capped sticks.

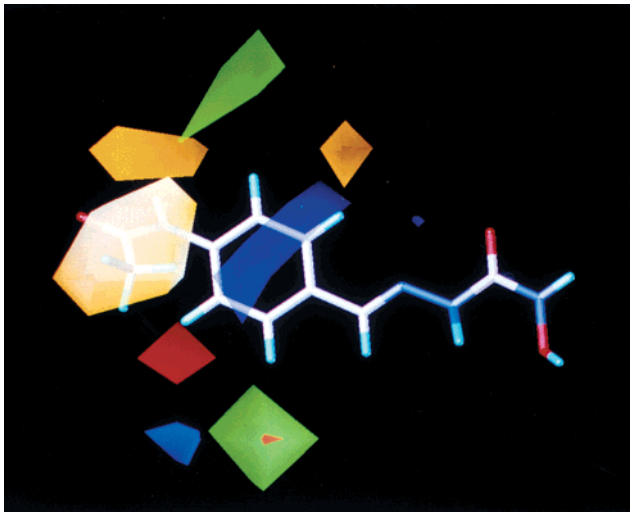

Figure 3. CoMFA steric and electrostatic STDEV*COEFF contour plots of inactive compound **28**, from atom-based alignment with ClogP as additional descriptor (Analysis B). Sterically favored areas (contribution level 80%) are represented by green polyhedra. Sterically disfavored areas (contribution level 20%) are represented by yellow polyhedra. Positive charge favored areas (contribution level 80%) are represented by blue polyhedra. Negative charge favored areas (contribution level 20%) are represented by red polyhedra.

(Table 3). Since the contributions of HOMO and LUMO in all models were very low to be considered as significant, the model generated only with ClogP as an additional descriptor was chosen as the best CoMFA model, and the contours were analyzed using this model. The field values were calculated at each grid point as a scalar product of the associated QSAR coefficient, and the standard deviation of all values in the corresponding column of the data table (STDEV*COEFF) are plotted as the percentage contribution to the QSAR equation. The contour maps of the CoMFA model with atom-based alignment and ClogP as additional descriptor are shown in Figures 2 and 3.

CoMSIA. CoMSIA analysis was performed using steric, electrostatic, hydrophobic, and H bond donor and acceptor descriptors. Presently CoMSIA offers five different fields; therefore, 3D-QSAR models can be generated using the above fields in different combinations. To compare directly with CoMFA, only a few combinations were considered which are complimentary to previously generated CoMFA models. The rms alignment used for CoMFA study served as alignment to CoMSIA. The results of CoMSIA are summarized in Table 4. The CoMSIA models showed considerable correlative and predictive properties. Hence all the models are significant in terms of explaining the observed biological activity. In all the models, hydrophobic field was common factor indicating the importance of lipophilicity for the present series of molecules. The model generated using hydrophobic and H bond donor and acceptor descriptors has higher r^2_{cv} and r^2_{pred} than the rest of the models but has lower r^2_{ncv} and F values. Also the SEE is higher. Incorporation of all the fields resulted in the reduction of r^2_{cv}. Combination of steric, electrostatic, and hydrophobic descriptors yielded a model with proper balance of all the statistical terms. It has good predictive ability (r^2_{pred}) of 0.735. To check

Table 4. Results of CoMSIA Analysis[a]

	SEH	HDA	SEHDA	SEHD	SEHA
r^2_{cv}	0.627	0.683	0.591	0.621	0.592
SEP	0.490	0.452	0.514	0.514	0.513
components	4	4	4	4	4
r^2_{ncv}	0.930	0.880	0.993	0.927	0.932
SEE	0.212	0.278	0.208	0.217	0.210
F	63.427	34.909	65.803	60.450	64.704
r^2_{pred}	0.735	0.816	0.744	0.738	0.802
			Contribution		
steric	0.203	–	0.180	0.192	0.189
electrostatic	0.428	–	0.299	0.352	0.352
hydrophobic	0.369	0.509	0.277	0.294	0.331
donor	–	0.271	0.139	0.162	–
acceptor	–	0.220	0.105	–	0.128
r^2_{bs}	0.961	0.926	0.969	0.964	0.967
std dev	0.020	0.031	0.018	0.017	0.015

[a] S = steric, E = electrostatic, H = hydrophobic, D = donor, A = scceptor.

whether the addition of H bond donor or acceptor descriptors affect the model, each descriptor was considered along with steric, electrostatic, and hydrophobic descriptors for generating the model. It is observed that addition of an H bond donor did not affect the previous results, but addition of an acceptor caused reduction in r^2_{cv} (0.592), and the comparison of the individual contribution revealed that the donor surpasses the acceptor contribution, suggesting the of role of an H bond donor functional group for the biological activity. In CoMSIA, the model with steric, electrostatic, hydrophobic, and H bond donor fields was selected as the best model on the basis of presence of proper (1) statistical terms and (2) descriptors to explain the observed biological activity. The CoMSIA contour maps were shown in Figures 4−6. The best models of CoMFA and CoMSIA were further subjected for rigorous statistical cross-validation (using two and five groups) and randomization PLS analysis. The results are summarized in Table 5. As can be seen from the table r^2_{cv} of 0.490 and 0.634 for CoMFA and 0.422 and 0.560 for CoMSIA

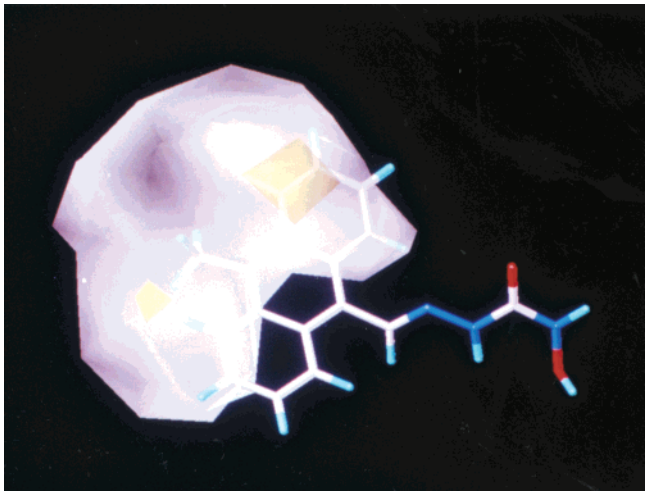

Figure 4. CoMSIA hydrophobic fields. Yellow polyhedra indicate regions where hydrophobic substituents are favored, while white polyhedra indicates hydrophobic disfavored region. Compound **21** is shown in capped sticks.

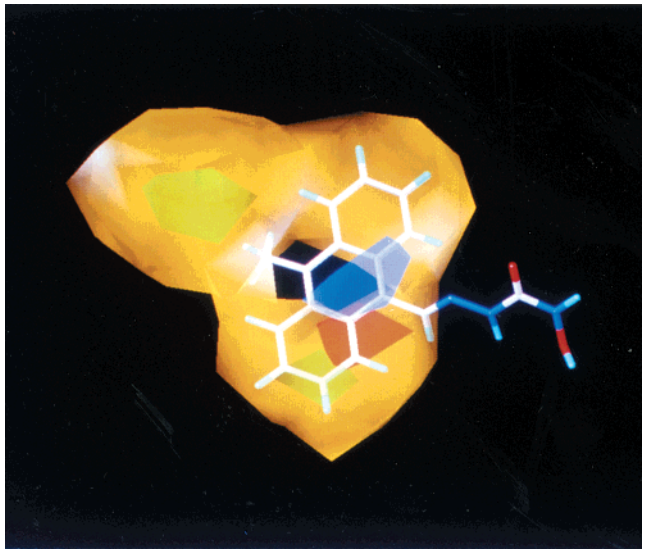

Figure 5. CoMSIA steric and electrostatic contour plots. Compound **21** is shown in capped sticks. Sterically favored areas (contribution level of 80%) are represented by green polyhedra. Sterically disfavored areas (contribution level of 20%) are represented by yellow polyhedra. Positive charge favored areas (contribution level of 80%) are represented as blue polyhedra, while positive charge disfavored areas (contribution level of 20%) are represented by red polyhedra.

with two and five groups, respectively, it is clear that models are stable and statistically robust. Negative r^2_{cv} values from a randomization method further consolidates that the models generated are not by chance correlation. The predicted activities of both training and test set molecules using the best CoMFA and CoMSIA models are given in Table 6.

Interpretation of QSAR Models. The present 3D-QSAR models were generated using 24 molecules as a training set in which hydroxyurea (HU), a commercially available RR inhibitor, was included. The resultant models of both CoMFA and CoMSIA have shown considerable internal and external predictive properties, indicating HU fits well into the equation. The authors in the original synthetic paper have mentioned that the compounds may act as antitumor agents by acting on

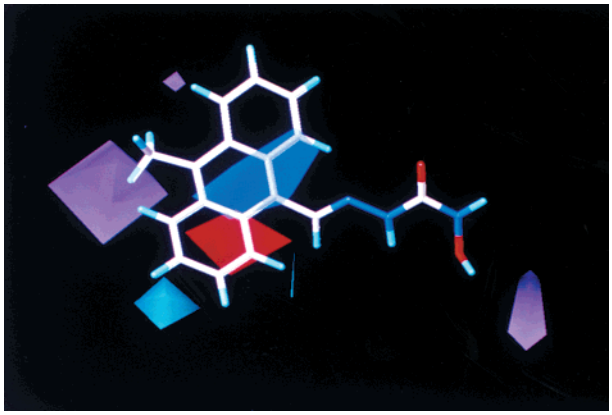

Figure 6. CoMSIA Electrostatic and hydrogen bond donor contour plots. Compound **21** is shown in capped sticks. Positive charge favored areas (contribution level of 80%) are represented as blue polyhedra, while positive charge disfavored areas (contribution level of 20%) are represented by red polyhedra. Hydrogen bond donor favored areas (contribution level of 80%) are represented by cyan polyhedra and disfavored areas (contribution level of 20%) are represented by purple polyhedra.

Table 5. Summary of Analysis of Cross-validation and Randomized Biological Activities of CoMFA and CoMSIA Models Generated Using rms Alignment Method

	r^2_{cv}[a] CoMFA		r^2_{cv}[b] CoMSIA		r^2_{cv}[c]	
	two groups	five groups	two groups	five groups	CoMFA	CoMSIA
mean	0.490	0.634	0.422	0.560	−0.168	−0.247
std dev	0.136	0.109	0.127	0.080	0.300	0.319
high	0.731	0.752	0.709	0.660	0.245	0.254
low	0.234	0.329	0.153	0.340	−0.904	−0.835

[a] Cross-validation using two and five groups with optimum number of components, average of 25 runs using ClogP as an additional descriptor. [b] Cross-validation using two and five groups with optimum number of components, average of 25 runs using steric, electrostatic, hydrophobic, and hydrogen bond donor fields. [c] Cross-validated r^2 with randomized biological activities, average of 25 runs.

the RR enzyme. Their assumption was based on the fact that the presence of an established pharmacophore (RNC(=O)NHOH), which is also present in HU, may induce RR inhibition.[11] In both CoMFA and CoMSIA models, the biological activity of HU (4.086) was predicted optimally (4.078 and 4.040 by CoMFA and CoMSIA, respectively, Table 6). The basic assumption of any QSAR method is that the mechanism of action of molecules considered for the generation of models must be the same. Hence, it can be considered that the mechanism of action of SB−HSC derivatives and HU is the same, i.e., the antitumor activity of SB−HSC may be due to RR enzyme inhibition.

Out of the different models generated (Table 2) using steric and electrostatic fields in CoMFA method, none of them gave statistically significant models. The inclusion of ClogP gave the best CoMFA model, suggesting that for the current series of molecules apart from steric and electrostatic interactions, lipophilicity is necessary for antitumor activity to enable the molecules to reach the site of action. Since molecules considered for the present study contain diverse functional groups representing polar, nonpolar, and H bond donor and acceptor properties, we thought to explore their influence on the antitumor activity. Hence, we additionally incorporated

Table 6. Predicted Antitumor Activities of Molecules Used in the Present Study from Best CoMFA and CoMSIA Model[a]

	predicted pIC_{50}	
compound	CoMFA (S, E, ClogP)	CoMSIA (S, E, H, D)
1	5.160	5.161
2	4.872	4.740
3	5.223	5.149
4	4.880	4.760
5	4.150	3.754
6	5.289	5.291
7	3.685	3.727
8	3.374	3.635
9	3.480	3.243
10	3.399	3.536
11	4.544	4.373
12	4.285	4.211
13	4.266	4.506
14	4.361	4.435
15	3.857	4.022
16	3.195	3.289
17	3.074	3.477
18	3.334	3.181
19	4.601	4.368
20	4.484	4.603
21	5.284	5.176
22	3.608	3.428
23	5.344	5.334
24	4.078	4.040
25*	3.877	3.868
26*	3.826	3.457
27*	4.020	3.985
28*	3.203	3.519

[a] S = steric, E = electrostatic, H= hydrophobic, D = donor. *Test set molecules.

HOMO and LUMO properties of the molecules in the QSAR studies. Addition of HOMO or LUMO individually to CoMFA fields yielded models with proper r^2_{cv} and lower r^2_{pred}, but either of them in combination with ClogP yielded statistically acceptable models. The combination of CoMFA fields, HOMO, and ClogP predicted the test set slightly better than the model of combination of CoMFA fields, LUMO and ClogP. This observation hints that compounds with proper lipophilicity and H bond donor functional groups may be associated with increased enzyme inhibition, in turn, the antitumor activity. It is found in the literature that RR inhibitors containing the NH(C═O)NHOH functional group inhibit the enzyme by one-electron transfer from the functional group to the tyrosyl free radical group.[24] Therefore, if the compounds contain additional functional groups, such as OH or OCH_3 (hydrogen bond donor), they may also act as free radical scavengers or iron chelators. It is evident from the SAR that molecules with hydrogen bond donor groups showed increased activity. Though we have selected a model composed of steric, electrostatic, and ClogP fields, the contribution of HOMO should also be considered.

In case of CoMSIA, as observed with CoMFA models, with (1) steric, electrostatic, and hydrophobic fields, (2) steric, electrostatic, hydrophobic, and H bond donor fields gave significant statistical parameters. The presence of a hydrophobic field in both models justifies the lipophilic requirement of molecules for better activity. Presence of an H bond donor descriptor suggests that an H bond donor functional group may lead to enhanced activity.

In both methods the lipophilic term reflects its importance for antitumor activity. The same has been demonstrated in the initial SAR and QSAR studies.[11] Thus, both methods clearly explain the mechanism of action of SB−HSC derivatives.

Visualization of 3D Contour Maps. CoMFA. To visualize the information content of the derived 3D-QSAR models, CoMFA contour maps were generated by interpolating the products between the 3D-QSAR coefficients and their associated standard deviations. Figure 2 shows the CoMFA contour map from the analysis based on rms alignment using the most active molecule as a reference structure. The green contours represent the regions of high steric tolerance, while yellow contours represent regions of unfavorable steric effects. The sterically favored green contour can be found in the figure around the anthracene ring. The most active compound, which has anthracene nucleus, i.e., the pharmacophore bearing central ring, is fused with two aromatic rings, which are accommodated within the sterically favored region. Therefore, compounds with larger substitution on the pharmacophore-bearing ring is essential for high activity, e.g., compounds **2**, **3**, **4**, and **6** are highly active because they contain bulkier halo groups, which are oriented within the favorable green contour. This suggests that the bulk and electronegative nature of a compound may offer favorable steric interactions at the active site. The favorable green regions are followed by unfavorable yellow regions, suggesting that substituents and the orientation of the ring bearing the pharmacophore are important for activity.

The blue contours (Figure 2) describe regions where a positively charged group enhances activity. The electrostatic contour plots, which are localized around the phenyl ring, suggest that substitutions on this ring indicate the electrostatic interactions of the compounds. A large blue region overlapping the central aromatic ring, which emphasizes the necessity of positively charged group for activity, justifies that hydroxysemicarbazide is an essential pharmacophore for antitumor activity. Small negatively charged (electron-rich) favorable red regions found at ortho- and meta-positions specify that an electron-rich substituent enhances the activity. These regions support the observation that OH (hydrogen donor/electron-rich system) substitution at the ortho-position enhances the antitumor activity. The electron-rich substitution at the meta-position leads to increased activity. The presence of red contour regions at meta- and ortho-positions and sterically favorable regions at the other meta-position hints that compounds with adjacent ortho-substitution, preferably OH, and a sterically bulky electronegative functional group at other meta-position may lead to more active compounds.

The least active compound, which has a substitution ($NHCOCH_3$) para to the essential pharmacophore of the aromatic ring, is shown in the Figure 3. The acetyl group is oriented in a sterically unfavorable yellow contour, which may lose important interactions at the active site, and will be detrimental to activity. Therefore, the nature of substitution at para-position is sensitive and not uniform and may not be essential for activity. This is further supported by the fact that compounds substituted by functional groups at this position showed moderate to less activity (compounds **6** and **8**). Overall, the CoMFA contour maps not only explain the SAR of

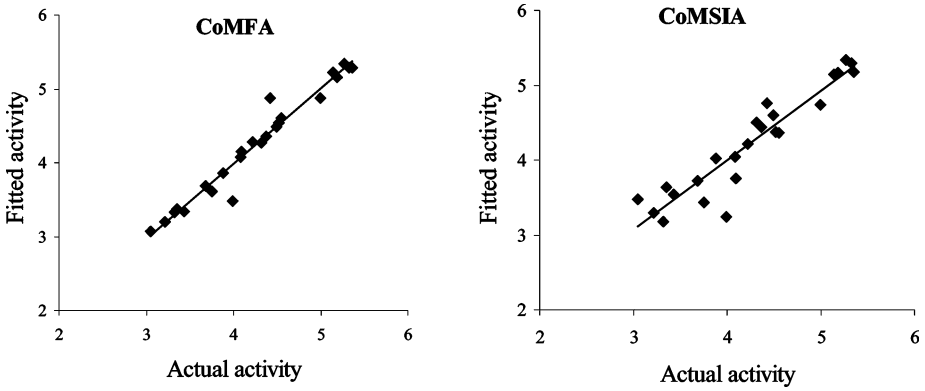

Figure 7. Fitted vs actual activity values for CoMFA and CoMSIA analysis of the training set.

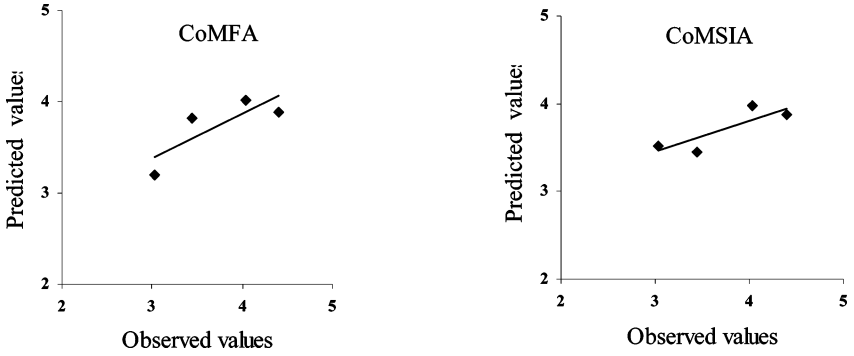

Figure 8. Predicted vs observed activities for CoMFA and CoMSIA analysis of the test set.

molecules as reported by the Ren et al., but also provide useful guidelines toward designing compounds for better activity.

CoMSIA. Figures 4−6 show the CoMSIA contour maps with the most active molecule. Analysis of CoMSIA hydrophobic contour maps (Figure 4) indicates that the lipophilic favorable yellow region is found below the aromatic ring followed by lipophilic unfavorable white contour surrounding the anthracene nucleus. This indicates that an optimum lipophilicity is essential for antitumor activity. The steric contour maps of CoMSIA are also similar to CoMFA steric maps (Figure 5). The interesting feature of CoMSIA method is that it provides contour maps of H bond donor fields separately. The electrostatic and H bond donor contour maps are shown in Figure 6. In CoMSIA, red polyhedra covering ortho- and meta-positions indicate the presence of electron-rich functional groups at these positions to enhance biological activity. As seen in CoMFA, the CoMSIA also shows big blue polyhedra over the ring-bearing pharmacophore, which signifies the importance of hydroxysemicarbazide functional group. In the present study the H bond donor field provides further support to substitution by electron-rich groups at ortho- and meta-positions for better activity. The presence of H bond donor favorable cyan contours at ortho- and meta-positions support the above assumptions. H bond donor unfavorable purple polyhedra observed at the para-position indicate the presence of electron-rich functional groups detrimental to activity.

CoMFA vs CoMSIA. Comparisons of the models derived from both CoMFA and CoMSIA were made to (1) assess their predictive abilities, (2) to gain insights into the observed variance in activity, and (3) to suggest a putative mechanism of action. The CoMSIA method apart from steric and electrostatic fields (as in CoMFA) additionally provides hydrophobic and H bond donor and acceptor fields. To compare CoMFA with CoMSIA, in the present study the CoMFA was run with additional descriptors (ClogP, HOMO, and LUMO) which are complimentary to the additional fields of CoMSIA, respectively.

We have selected the CoMFA model containing additional descriptor ClogP which gave r^2_{cv}, 0.708, r^2_{ncv}, 0.993, and r^2_{pred}, 0.796. Though the model generated using steric, electrostatic, and hydrophobic fields in CoMSIA is the best model from the other models, we opted for the model containing an H bond donor in addition to steric, electrostatic, and hydrophobic fields. The selected model has an r^2_{cv} of 0.621, less than the corresponding CoMFA model, and an r^2_{ncv} of 0.927 and r^2_{pred} of 0.738 (almost similar to that of CoMFA model). The graph depicting the calculated vs observed activities of training and test set molecules are shown in Figures 7 and 8, respectively. A bootstrapped r^2 (r^2_{bs}) of 0.998 and 0.964 for CoMFA and CoMSIA model, respectively, further support the significance of the selected models. These facts pinpoint that for the current series of molecules, both CoMFA and CoMSIA are complimentary to each other in statistical terms. The contour maps generated from both models not only are similar but also clearly explain the influence of variation in the structural features over the observed biological activity. Hydroxyurea (HU), a known RR inhibitor, was used successfully for generating the models and was predicted optimally with a similar range in both methods. Thus, both studies suggest a common mechanism of action for HU and SB-HSC derivatives. On the basis of these observations, it can be confirmed that RR is a molecular target for antitumor activity of SB−HSC

derivatives. The presence of lipophilic (ClogP in CoMFA and hydrophobic field in CoMSIA) terms in the models of both methods suggests that antitumor activity of SB−HSC derivatives is primarily influenced by optimum lipophilicity necessary for improved bioavailability and binding affinity.

All the contour analyses suggest that the binding of molecules possessing structurally diverse substituents is driven by the hydrophobic groups, which should be optimum in 3D-space. Both models urge the importance of substitution at the ortho- and meta-position by electron-rich groups for improved therapeutic efficacy.

Conclusions

The 3D-QSAR methods, CoMFA and CoMSIA, have been applied to a set of recently described SB−HSC derivatives as antitumor agents. The models obtained using these methods showed high correlative and predictive abilities. A high bootstrapped r^2 value and small standard deviations indicate that a similar relationship exists in all compounds. The compounds considered for the study have antitumor activity against L1210 cancer cells. It is believed that due to the presence of an essential pharmacophore for RR inhibition the compounds have shown antitumor activity, which was not supported by any experimental evidence. Hence, to understand and find a possible mechanism of action, we included a standard RR inhibitor, hydroxyurea (HU), in the study, and consequently models were generated. In both methods the HU fitted well, indicating existence of a similar mechanism of action between HU and SB−HSC derivatives, i.e., inhibition of the RR enzyme for antitumor activity.

Inclusion of additional descriptors, such as ClogP, improved the statistical significance of the model, indicating lipophilicity may contribute to pharmacokinetic/pharmacodynamic profiles of the molecule and help to enhance the antitumor activity. Out of the three methods of alignment considered, rms fit along with ClogP resulted in the best CoMFA model. The same alignment was also considered for CoMSIA where all five fields were considered in different combinations. The model generated using steric, electrostatic, hydrophobic, and H bond donor fields gave a statistically significant model and provided proper meaning for observed biological activity. The contour maps of both methods were similar in explaining the influence of substitutions on antitumor activity. It is observed from the contour maps of both methods that substitution by electron-rich functional groups at the ortho- and meta-position(s) may improve pharmacological effects of the compounds. The generated models not only explain the SAR but also exhibited good external predictivity, which makes any QSAR study a significant one. The suggested mechanism of action and the structural requirements identified through the contour maps are consistent with the findings of Ren et al., which may help in designing new RR inhibitors as antitumor agents.

Acknowledgment. We gratefully acknowledge support for this research from the University Grants Commission (UGC), New Delhi, under its DSA and COSIST programs. A.V.R. is grateful to RPG-Life Sciences, Navi Mumbai, for the award of senior research fellowship. A.V.R. also thanks Purushottamachar P., Vishal V. Kulkarni, and Prashant S. Kharkar for useful discussions.

References

(1) Lien, E. J. Ribonucleotide Reductase Inhibitors as Anticancer and Antiviral Agents. *Prog. Drug Res.* **1987**, *31*, 1−26.
(2) Nocentini, G. Ribonucleotide Reductase Inhibitors: New Strategies for Cancer Chemotherapy. *Crit. Rev. Oncol. Hematol.* **1996**, *22*, 89−126.
(3) Koneru, P. B.; Lien, E. J.; Avramis, V. I. Synthesis and Testing of New Antileukemic Schiff Bases of N−Hydroxy-N′-aminoguanidine Against CCRF−CEM/0 Human Leukemia Cells In Vitro and Synergism Studies with Cytarabine (Ara-C). *Pharm. Res.* **1993**, *10*, 515−520.
(4) Cory, J. G.; Cory, A. H. *Inhibitors of Ribonucleotide Diphospahte Reductase Activity*; Pergamon Press: New York, 1989.
(5) Van't Riet, B.; Wampler, G. L.; Elford, H. L. Synthesis of Hydroxy- and Amino-Substituted Benzohydroxamic Acids: Inhibition of Ribonucleotide Reductase and Antitumor Activity. *J. Med. Chem* **1979**, *22*, 589−592.
(6) Das, A.; Trousdale, M. D.; Ren, S. J.; Lien, E. J. Inhibition of Herpes Simplex Virus Type 1 and Adenovirus Type 5 by Heterocyclic Schiff Bases of Aminohydroxy-guanidine Tosylate. *Antiviral Res.* **1999**, *44*, 201−208.
(7) Navarra, P.; Preziosi, P. Hydroxyurea: New Insights on an Old Drug. *Crit. Rev. Oncol. Hematol.* **1999**, *29*, 249−255.
(8) Finch, R. A.; Liu, M.; Grill, S. P.; Rose, W. C.; Loomis, R.; Vasquez, K. M.; Cheng, Y.; Sartorelli, A. C. Triapine. (3-Aminopyridine-2-Carboxaldehyde-thiosemicarba-zone): A Potent Inhibitor of Ribonucleotide Reductase Activity with Broad-Spectrum Antitumor Activity. *Biochem. Pharmacol.* **2000**, *59*, 983−991.
(9) Szekeres, T.; Fritzer-Szekeres, M.; Elford. H. L.. The Enzyme Ribonucleotide Reductase: Target for Antitumor and Anti-HIV Therapy. *Crit. Rev. Clin. Lab. Sci.* **1997**, *34*, 503−528.
(10) *Physicians' Desk Reference*, 51st ed.; Medical Economics Company, Inc.: Montvale, NJ, 1999; pp 774−781.
(11) Ren, S.; Wang, R.; Komatsu, K.; Bonaz-Krause, P.; Zyrianov, Y.; McKenna, C. E.; Csipke, C.; Tokes, A. Z.; Lien, E. J. Synthesis, Biological Evaluation and Quantitative Structure−Activity Relationship Analysis of New Schiff Bases of Hydroxysemi-carbazide as Potential Antitumor Agents. *J. Med. Chem.* **2002**, *45*, 410−419.
(12) Kulkarni, S. S.; Kulkarni, V. M. Three-Dimensional Quantitative Structure−Activity Relationship of Interleukin 1-β Converting Enzyme Inhibitors: A Comparative Molecular Field Analysis Study. *J. Med. Chem.* **1999**, *42*, 373−380.
(13) Gokhale, V. M.; Kulkarni, V. M. Comparative Molecular Field Analysis of Fungal Squalene Epoxide Inhibitors. *J. Med. Chem.* **1999**, *42*, 5348−5358.
(14) Kharkar, P. S.; Gaveria, H.; Varu, B.; Loriya, R.; Naliapara, Y.; Shah, A.; Kulkarni, V. M. Three-Dimensional Quantitative Structure−Activity Relationship of 1,4-Dihydropyridines as Antitubercular Agents. *J. Med. Chem.* **2002**, *45*, 4858−4867.
(15) Cramer, R. D., III; Patterson, D. E.; Bunce, J. D. Comparative Molecular Field Analysis (CoMFA) 1. Effect of Shape on Binding of Steroids to Carrier Proteins. *J. Am. Chem. Soc.* **1998**, *110*, 5959−5967.
(16) Talele, T. T.; Kulkarni, S. S.; Kulkarni, V. M. Development Of Pharmacophore Alignment Models as Input for Comparative Molecular Field Analysis of a Diverse Set of Azole Antifungal Agents. *J. Chem. Inf. Comput. Sci.* **1999**, *39*, 958−966.
(17) Murthy, S. V.; Kulkarni, V. M. 3D-QSAR CoMFA and CoMSIA on PTP 1B Inhibitors. *Bioorg. Med. Chem.* **2002**, *10*, 2267−2282.
(18) Gohlke, H.; Klebe, G. Drug Score Meets CoMFA: Adaptation of Fields for Molecular Comparison (AFMoC) or How to Tailor Knowledge-Based Pair-Potentials to a Particular Protein. *J. Med. Chem.* **2002**, *45*, 4153−4170.
(19) Cramer, R. D., III. Topomer CoMFA: A Design Methodology for Rapid Lead Optimization. *J. Med. Chem* **2003**, *46*, 374−388.
(20) Klebe, G.; Abraham, U.; Meitzner, T. Molecular Similarity Indices in A Comparative Analysis (CoMSIA) of Drug Molecules to Correlate and Predict their Biological Activity. *J. Med. Chem.* **1994**, *37*, 4130−4146.
(21) SYBYL 6.6, Tripos Associates: 1669, S. Hanley Road. Suite 303, St. Louis, MO 63144-2913.
(22) MOPAC. 6.0; Quantum Chemical Program Exchange: Indiana University No. 455.
(23) Dewar, M. J. S.; Zoebisch, E. G.; Healy, E. F.; Stewart J. J. P. AM1; A New General-Purpose Quantum Mechanical Molecular Model. *J. Am. Chem. Soc.* **1985**, *107*, 3902−3909.
(24) Libermann, B.; Lassmann, G.; Langen, P Quenching of Tyrosine Radicals of M2 Subunit from Ribonucleotide Reductase in Tumor Cells by different Antitumor Agents: An EPR Study. *Free Radical Biol. Med.* **1990**, *9*, 1−4.

JM030016A